Communication

Diameter-Dependent Surface Photovoltage and Surface State Density In Single Semiconductor Nanowires

Afsoon Soudi, Cheng-Han Hsu, and Yi Gu

Nano Lett., **Just Accepted Manuscript** • Publication Date (Web): 17 Sep 2012

Diameter-Dependent Surface Photovoltage and Surface State Density In Single Semiconductor Nanowires

A. Soudi, C.-H. Hsu, and Y. Gu*

Department of Physics and Astronomy, Washington State University, Pullman, WA 99164

Based on single-nanowire surface photovoltage measurements and finite-element electrostatic simulations, we determine the surface state density, N_s, in individual n-type ZnO nanowires as a function of nanowire diameter. In general, N_s increases as the diameter decreases. This identifies an important origin of the recently reported diameter dependence of the surface recombination velocity, which has been commonly considered to be independent of the diameter. Furthermore, through the determination of the surface carrier lifetime, we suggest that the diameter dependence of the surface state density accounts for the rather abrupt transition from bulk-limited to surface-limited carrier transport over a narrow nanowire diameter regime (~ 30 – 40 nm). These findings are supported by the comparison between bulk-limited and surface-dependent minority carrier diffusion lengths measured at various diameters.

Keywords: Surface States; Surface Photovoltage; Nanowires; Carrier Transport

* Corresponding author. Email: yigu@wsu.edu

Charge carrier transport plays a central role in semiconductor-based device operations. The minority carrier transport is particularly important, as it controls the majority carrier transport and thus the current characteristics in p-n junctions, a fundamental element in many semiconductor devices including solar cells, photodetectors, light emitting diodes, and lasers. With the device dimension decreasing in the nanometer regime, surface effects become a significant factor in limiting carrier transport. In semiconductor nanowires, which are being extensively explored for photovoltaics[1, 2] and opto-electronics,[3-5] surface effects on carrier transport are often manifested through carrier trapping and electron-hole recombination at surface states. As the diameter decreases, this surface-facilitated carrier recombination becomes to dominate over the recombination process in the bulk, and thus limit the minority carrier lifetime and diffusion length. Carrier recombination at the surface is usually described by the surface recombination velocity, *S*, which is proportional to the surface state density and the carrier capture cross section. *S* has been assumed to be a constant quantity independent of the nanowire diameter,[6] and the increasing dominance of the surface effects on carrier transport has been commonly explained by the increasing surface-to-volume ratio as the diameter decreases.

Recent studies,[7,8] however, have suggested that the surface-to-volume ratio alone significantly underestimates the significance of surface effects at small diameters. Particularly, the transition from bulk-limited to surface-limited carrier transport occurs over a narrow diameter regime (~ 30 – 40 nm),[8] which cannot be accounted for by only the variations of the surface-to-volume ratio within this regime. Correspondingly, these studies indicate a diameter-dependent *S* that increases with the decreasing diameter in Si and ZnO nanowires.[9, 10] A study of the photoluminescence lifetime in ZnO nanowires also indicates a diameter-dependent *S*,[6] although this was not explicitly pointed out. The origin of this diameter dependence of *S* remains unclear. Here, using

single-nanowire surface photovoltage measurements, we directly determine the surface barrier height in single n-type ZnO nanowires. By coupling these results to finite-element electrostatic simulations, we obtain the acceptor-type surface state density and the minority carrier surface lifetime as functions of the nanowire diameter. These results identify an important origin of the diameter-dependent *S* and account for the abrupt transition from bulk-limited to surface-limited minority carrier transport as the diameter decreases. These findings are further supported by the measurement of bulk-limited minority carrier diffusion length in the presence of strong surface effects, which enables a direct view of the significance of surface effects as a function of diameter through a comparison to the surface-dependent minority carrier diffusion length.

ZnO nanowires were grown by a catalytic chemical vapor deposition (CVD) method, as described previously.[11] Single-crystal wurtzite-structure nanowires were obtained, and no extended lattice defects were observed by transmission electron microcopy.[9] The growth direction of these nanowires is along the [0001] direction.[9] Nanowires with different diameters were obtained under the same growth conditions, and thus no diameter dependence of the unintentional impurity incorporation was expected. These nanowires are unintentionally n-type doped, with an electron mobility of ~ 90 – 100 cm^2/Vs and an electron density of ~ 10^{17} cm^{-3} determined from electrical measurements.[8] The electron mobility and density are comparable to those reported in high-quality CVD-grown ZnO nanowires.[12-15] For surface photovoltage measurements, ZnO nanowires were deposited on Si substrates coated with a 200 nm-thick Si_3N_4 layer, and e-beam lithography followed by metallization and life-off processes were used to define metal electrodes on single nanowires. The surface potential of single nanowires was measured by scanning Kelvin probe force microscopy (KPFM) with the global optical excitation provided by the 325 nm emission from a He-Cd laser; these experiments were carried out in

ambient air, with the schematics shown in Fig. 1 (b). Pt-coated probes (ATEC, Nanosensors) with the nominal radius less than 20 nm were used for the KPFM experiments; details can be found in Ref. 10. Three-dimensional finite-element electrostatic simulations (see also below for details) were implemented using a commercial software (*Synopsys* TCAD *Sentaurus*).

The origin of surface photovoltage (SPV) is illustrated in Fig. 1 (a) for an n-type semiconductor nanowire under a low-level optical illumination. Specifically, acceptor-like surface states, when occupied by electrons, carry negative charges, and induce the upward surface band bending as well as a surface depletion of electrons in the semiconductor. Under an above-bandgap optical excitation, negatively charged surface states capture the photogenerated holes (which are minority carriers in this case) and become neutral, and this reduces the surface band bending.[16] SPV is defined as the changes in the surface potential due to this optical illumination. When most of the surface states are neutralized, the surface band bending disappears; in this case, the SPV approaches the maximum value (i.e. photosaturation), which is of the same magnitude as the surface potential barrier height at equilibrium (in the dark). This approach to measuring the surface potential barrier height has been widely used in characterizing surface properties of various bulk and thin-film semiconductors[17-19] (see also Supporting Information for potential issues of this approach).

Figures 2 (b) and (c) show the surface potential maps of a ZnO nanowire in the dark and under the optical illumination, respectively. With the carrier lifetime in ZnO on the order of hundreds of ps, the maximum optical power density (~ 0.3 Wcm^{-2}) used in this study leads to a photogenerated free carrier concentration of ~ 10^{13} – 10^{14} cm^{-3}. This is much lower than the equilibrium electron density (~ 10^{17} cm^{-3}) in our ZnO nanowires, and thus corresponds to the low-level optical excitation condition. By considering the work functions of Pt (KPFM probe)

and ZnO, the observed increase in the surface potential under the optical excitation, i.e. a positive SPV as shown in Figs. 2 (b) and (c), indicates a decrease in the work function of the ZnO surface. This is consistent with a lowering of the upward surface band bending, as shown in Fig. 1 (c).[20] This surface band bending at equilibrium is due to the presence of acceptor-type surface states. We note that the interaction between chemisorbed oxygen molecules and ZnO surface atoms leads to acceptor-type surface states with the energy, E_s, at ~ 0.7 – 0.9 eV below the conduction band.[21] In addition, intrinsic acceptor-type surface states have also been reported at energy levels of 0.38 – 0.5 eV above the valence band.[22, 23] Other surface adsorbates including hydrogen and hydroxyl groups can also play a role in surface state formation.[24] Among these, the oxygen-induced surface states have been shown to be the dominant species in ambient air in ZnO nanowires,[25] and thus will be the focus of this study. These acceptor-type states, usually occupied by electrons as their energy levels are below the Fermi level in n-type ZnO under equilibrium, can capture photogenerated holes and thus play an important role in limiting hole transport.

The surface barrier height at equilibrium can be obtained from the SPV under photosaturation conditions. The SPV was measured away from the metal junction, where the SPV is constant along the nanowire. Figure 2 (d) shows the SPV (solid circles) as a function of the optical excitation intensity. A saturation of SPV towards ~ 0.23 V can be observed. We note that the photosaturation occurs under low-level optical excitations. This suggests that the direct modification, specifically the neutralization, of negatively charged surface states is the main mechanism for the observed SPV and photosaturation, as opposed to the screening of the surface charges by photogenerated carriers.[26, 27] As discussed above, the saturation value of SPV can be taken as the surface barrier height under equilibrium.[28] Using this approach, the surface barrier

height was obtained in nanowires with various diameters, and the results (solid circles) are shown in Fig. 2 (e). In general, the surface barrier height increases with the decreasing diameter. To relate this result to the surface state density, we calculated the surface barrier height as a function of surface state density, N_s, for various nanowire diameters. The simulations were conducted for the nanowires at equilibrium (i.e. in the dark). Particularly, the three-dimensional Poisson's equation is given by

$$\nabla^2\varphi = -\frac{q}{\epsilon}(p - n + N_D^+) \quad (1)$$

With the charge neutrality condition, we have

$$\int(p - n + N_D^+)dV = \int N_s^- dA \quad (2)$$

where N_s^- is the density of the electron-occupied surface states, which carry negative charges. The left side of the Equation (2) represents the total positive volume charges inside the nanowire, with the right side of the equation as the total negatively-charged (electron-occupied) surface states on the nanowire surface. The surface states are assumed to be distributed uniformly on the nanowire surface. The negatively charged surface state density, N_s^- , is related to the density of the total surface states, N_s, the Fermi-Dirac statistics. Equations (1) and (2) were solved together with the charge continuity equations at equilibrium

$$\frac{1}{q}\vec{\nabla}\cdot\left(q\mu_n n\vec{\varepsilon} + qD_n\vec{\nabla}n\right) = -\frac{1}{q}\vec{\nabla}\cdot\left(q\mu_p p\vec{\varepsilon} + qD_p\vec{\nabla}p\right) = 0 \quad (3)$$

in a self-consistent manner.

Table I lists the material parameters used in the calculation. The electron and hole diffusivities, D_n and D_p, are calculated as $(kT/q)\mu_n$ and $(kT/q)\mu_p$, respectively. A donor activation energy of 46

meV was used for the calculation; this value corresponds to hydrogen donors,[29, 30] the dominant shallow donor species in ZnO, and is also consistent with the value extracted from variable-temperature electrical measurements of ZnO nanowires.[31] Fermi-Dirac statistics was used to calculate the free electron density, which is close to the effective density of states of the conduction band in ZnO (~ 3×10^{18} cm^{-3}). For the simulations, the ZnO nanowire was encapsulated by ambient air [Fig. 3 (a)], and the surface states were defined at the nanowire/air interface.

Figures 3 (b) and (c) show the calculated cross-sectional distributions of the electrostatic potential and free electron density in a 27 nm-diameter nanowire. In this case, N_s and E_s are 4.1 × 10^{12} cm^{-2} and 0.9 eV (which corresponds to chemisorbed oxygen-related surface states) below the conduction band, respectively. As expected, the presence of acceptor-type surface states leads to the surface band bending and depletion of electrons near the surface. With the surface barrier height as a function of N_s obtained through the simulation, as shown in Fig. 3 (d), the value of N_s can be determined for the measured surface barrier height. We note that the uncertainty on E_s does not affect the determination of N_s, as shown in Fig. 3 (d) for E_s of 0.7 eV and 0.9 eV. This is true if the value of E_s is large than the measured surface barrier energy (0.15 – 0.3 eV), i.e. the surface state energy levels are significantly below the conduction band, because in this case the electron occupation of surface states is independent of surface band bending. For the 27 nm-diameter nanowire, the experimentally measured surface barrier height (~ 0.29 V) corresponds to an N_s of 4.1 × 10^{12} cm^{-2}. As a verification of the simulation results, the average free electron density with the N_s given by 4.1 × 10^{12} cm^{-2} was calculated to be ~ 2 × 10^{17} cm^{-3} from Fig. 3 (c), for a given total donor concentration (10^{19} cm^{-3}). This agrees well with the value experimentally estimated from electrical measurements (~ 10^{17} cm^{-3}).[8]

N_s as a function of nanowire diameter, plotted as solid squares in Fig. 3 (e), in general, shows an increase in N_s as the diameter decreases. This identifies an important origin of the diameter dependence of S, which is given by $N_s\sigma v_{th}$, with σ and v_{th} being the carrier capture cross section and thermal velocity, respectively. Further insights into the role of the diameter dependence of N_s in surface effects on minority carrier transport can be obtained by considering the following relation:[32]

$$\frac{1}{\tau_{\text{eff}}} = \frac{4\beta^2 D_p}{d^2} + \frac{1}{\tau_{\text{B}}} \quad (3)$$

with β given by:

$$\beta J_1(\beta) = \frac{dS}{2D_p} J_0(\beta) \quad (4)$$

where τ_{eff} is the effective hole lifetime, τ_{B} is the hole lifetime in bulk ZnO, and d is the nanowire diameter. The diameter dependence of τ_{eff} is the controlling factor for the hole diffusion length, L_{D}, which is given by $\sqrt{D_p \tau_{\text{eff}}}$. The first term on the right side of equation (3) can be considered as an effective lifetime controlled entirely by surface effects, i.e. the surface lifetime, $\tau_{\text{sur}} = \frac{d^2}{4\beta^2 D_p}$. With the known N_s and σ (which is given by 10^{-16} cm^{-2} for oxygen-induced surface states[33]), τ_{sur} can be calculated as a function of nanowire diameter, and the results are plotted as solid circles in Fig. 3 (f). The corresponding τ_{eff} was then obtained from equation (3) with τ_{B} taken to be 150 ps,[34] and is plotted in Fig. 3 (f). The relative significance of surface effects is indicated by the comparison between τ_{sur} and τ_{B}: when τ_{sur} is smaller (larger) than τ_{B}, the hole transport is limited by surface (bulk) effects. As shown in Fig. 3 (f), τ_{sur} becomes smaller than τ_{B}

at the diameter of ~ 35 nm, and this is consistent with the previously reported transition from bulk-limited to surface-limited carrier transport in the 30 – 40 nm diameter regime.[11]

This diameter dependence of N_s indicates changes in the surface electronic structure as the diameter varies. Theoretical studies[35, 36] have suggested an increase in the mid-bandgap surface states in wurtzite-structure nanowires and quantum wells as the diameter and well thickness decrease. Such a trend was attributed to the coupling of surface wave functions on identical surfaces, e.g. the six $(1\bar{1}00)$ side surfaces in [0001] oriented nanowires. Particularly for wurtzite GaN nanowires, this effect was calculated to become significant as the diameter decreases below 40 nm. Another possible origin of the observe phenomena might be the surface reconstruction in nanowires. As shown by simulations reported in Ref. 37, ZnO nanowires with different diameters exhibit different atomic displacements on the surfaces due to surface reconstructions. This was used to explain a diameter dependence of the Young's modulus in the diameter range of 20 nm to 80 nm. The difference in the surface atomic displacements might lead to different surface electronic structures. In addition, previous experimental studies have shown changes in the x-ray near-edge absorption spectra in ZnO nanowires with various diameters,[38] which indicate variations of the surface electronic properties as a function of diameter. While the exact nature of the changes in the surface electronic structure remains unclear, such changes are likely to modify the interactions between chemisorbed oxygen and surfaces, leading to a diameter-dependent N_s. We note that this diameter dependence of N_s might not be the only origin of the strong surface effects and the diameter-dependent S. As an example, modifications to the carrier capture cross section as the diameter varies might also contribute. Further studies including surface photovoltage spectroscopy measurements on single nanowires will provide more insights.

The comparison between τ_{sur} and τ_B, as well as the diameter dependence of τ_{eff}, shows that surface effects are minimal for diameters beyond 45 – 50 nm and are dominant for diameters smaller than 30 – 35 nm. This can be directly validated by measuring the bulk-limited L_D. Specifically, under the above-bandgap global optical excitation, the negatively charged acceptor-type surfaces states become neutralized, as shown schematically in Fig. 1. These hole-occupied surface states can no longer trap holes and facilitate the electron-hole recombination; therefore, the transport of the remaining free holes is limited by bulk-related processes. Figure 4 (a) shows the principle of measuring the bulk-limited L_D from the spatial variations of photogenerated free holes (Δp) under a global optical excitation. Particularly, a metal-semiconductor junction creates a gradient of Δp close to the space-charge region, which collects the holes. This gradient is characterized by a single exponential function exp (-x/L_D), with L_D in this case limited by the bulk effects.[39] This gradient of Δp can be related to the surface photovoltage (SPV) through the relation established in Ref. 40:

$$\mathrm{SPV}\ (\mathrm{x}) = C_0 \times \ln\left[1 + \frac{\Delta p}{C_2}\right] = C_0 \times \ln[1 + \frac{C_1 \times \exp\left(-\frac{\mathrm{x}}{L_D}\right) + \Delta \mathrm{p}_0}{C_2}] \quad (5)$$

where C_0, C_1, and C_2 are constants, and Δp_0 is the density of photogenerated free holes away from the space-charge region. The spatial variations of SPV close to the metal junction are controlled by L_D. By fitting the SPV spatial profile close to the metal junction using equation (5), the bulk-limited L_D can be extracted. One example is shown in Fig. 4 (b).[41] The comparison between bulk-limited and surface-dependent L_D, the latter of which was obtained by the near-field scanning photocurrent microscopy,[8] is shown in Fig. 4 (c). Consistent with the τ_{eff} being limited by bulk-related processes for large diameters, the surface-dependent L_D (open circles) is similar to the bulk-limited L_D (solid circles) for diameters larger than 40 nm. For smaller

diameters, an increasingly large difference between these two types of L_D points to more substantial surface effects. This evolution of the significance of the surface effects as a function of nanowire diameter agrees well with that indicated in Fig. 3 (f).

In summary, we have used KPFM to determine surface barrier height through surface photovoltage measurements in single ZnO nanowires. By considering the oxygen-induced surface states, which are the dominant surface species in ambient air in ZnO nanowires, we have estimated the corresponding surface state density based on the surface barrier height and finite-element electrostatic simulations. In general, the surface state density increases with decreasing diameter; this finding identifies an important origin of the recently reported diameter dependence of the surface recombination velocity. Through the determination of the carrier surface lifetime based on this result, we suggest that this diameter dependence of the surface state density contributes to the transition from bulk-limited to surface-limited carrier transport over a rather narrow diameter regime (30 – 40 nm). In addition, we have measured the bulk-limited minority carrier diffusion length, L_D, at various diameters, the comparison of which to the surface-dependent L_D enables a direct view of the significance of surface effects as a function of diameter. Our results provide important insights into surface effects on carrier transport in semiconductor nanostructures, and emphasize the need to consider mechanisms beyond the commonly used surface-to-volume ratio, e.g. possible modifications to the surface electronic structure, in understanding the significance of surface effects in general.

References:

1. Tian, B.; Kempa, T. J.; Lieber, C. M. *Chem. Soc. Rev.* **2009,** 38, 16-24.

2. Tang, J. Y.; Huo, Z. Y.; Brittman, S.; Gao, H. W.; Yang, P. D. *Nat Nanotechnol* **2011,** 6, 568-572.

3. Cho, C. H.; Aspetti, C. O.; Turk, M. E.; Kikkawa, J. M.; Nam, S. W.; Agarwal, R. *Nat Mater* **2011,** 10, 669-675.

4. Yan, R. X.; Gargas, D.; Yang, P. D. *Nat Photonics* **2009,** 3, 569-576.

5. Bertness, K. A.; Sanford, N. A.; Davydov, A. V. *IEEE J Sel Top Quant* **2011,** 17, 847-858.

6. Zhao, Q. X.; Yang, L. L.; Willander, M.; Sernelius, B. E.; Holtz, P. O. *J. Appl. Phys.* **2008,** 104, 073526.

7. Seo, M. A.; Dayeh, S. A.; Upadhya, P. C.; Martinez, J. A.; Swartzentruber, B. S.; Picraux, S. T.; Taylor, A. J.; Prasankumar, R. P. *Appl. Phys. Lett.* **2012,** 100, 071104.

8. Soudi, A.; Dhakal, P.; Gu, Y. *Appl. Phys. Lett.* **2010,** 96, 253115.

9. Soudi, A.; Lopez, R.; Dawson, R. D.; Gu, Y. *Appl. Phys. Lett.* **2009,** 95, 193111.

10. Soudi, A.; Aivazian, G.; Shi, S. F.; Xu, X. D.; Gu, Y. *Appl. Phys. Lett.* **2012,** 100, 033115.

11. Soudi, A.; Khan, E. H.; Dickinson, J. T.; Gu, Y. *Nano Lett.* **2009,** 9, 1844-1849.

12. Park, W. I.; Kim, J. S.; Yi, G. C.; Bae, M. H.; Lee, H. J. *Appl. Phys. Lett.* **2004,** 85, 5052-5054.

13. Chang, P. C.; Fan, Z.; Chien, C. J.; Stichtenoth, D.; Ronning, C.; Lu, J. G. *Appl. Phys. Lett.* **2006,** 89, 133113.

14. Chang, P. C.; Fan, Z. Y.; Wang, D. W.; Tseng, W. Y.; Chiou, W. A.; Hong, J.; Lu, J. G. *Chem. Mater.* **2004,** 16, 5133-5137.

15. Li, Q. H.; Liang, Y. X.; Wan, Q.; Wang, T. H. *Appl. Phys. Lett.* **2004,** 85, 6389-6391.

16. Some of the photogenerated electrons recombine with the holes, and the rest of them, as majority carriers, will be neutralized *via* the dielectric relaxation process if the semiconductor is connected to external electrodes/circuits.

17. Gopel, W.; Brillson, L. J.; Brucker, C. F. *J Vac Sci Technol* **1980,** 17, 894-898.

18. Adamowicz, B. *Surf. Sci.* **1990,** 231, 1-8.

19. Venger, E. F.; Kirillova, S. I.; Primachenko, V. E.; Chernobai, V. A. *Semiconductors* **1995,** 29, 121-126.

20. We note that, besides the changes in the surface barrier height, the Dember effect, originating from the spatially nonuniform distribution of photogenerated electrons and holes along the laser incident direction (the radial direction in nanowires), can also contribute to the SPV. However, the Dember effect requires a high-level optical excitation. Moreover, as the carrier diffusion length (see also the text) is larger than the ZnO nanowire diameter, the radial distribution of photogenerated carriers is expected to be relatively uniform. Therefore, the Dember effect is not expected to play a signifcant role.

21. Morrison, S. R. *Surf. Sci.* **1971,** 27, 586-604.

22. Prades, J. D.; Cirera, A.; Morante, J. R.; Comet, A. *Thin Solid Films* **2007,** 515, 8670-8673.

23. Teklemichael, S. T.; McCluskey, M. D. *Nanotechnology* **2011,** 22, 475703.

24. Woll, C. *Prog. Surf. Sci.* **2007,** 82, 55-120.

25. Lin, Y. H.; Wang, D. J.; Zhao, Q. D.; Li, Z. H.; Ma, Y. D.; Yang, M. *Nanotechnology* **2006,** 17, 2110-2115.

26. Aphek, O. B.; Kronik, L.; Leibovitch, M.; Shapira, Y. *Surf. Sci.* **1998,** 409, 485-500.

27. Kronik, L.; Shapira, Y. *Surf. Sci. Rep.* **1999,** 37, 1-206.

28. The surface potential measured by the KPFM is an average value over an effective area defined by the electrostatic interaction between the atomic force microscope (AFM) probe and the sample surface. Particularly, if the feature size, in our case the nanowire diameter, is significantly smaller than this effective area, then the measured surface potential is lower than the actual potential (e.g. Liscio, A.; Palermo, V.; and Samorì, P. *Adv. Funct. Mater*. **2008**, 18, 907–914). This effective area can be estimated from the point spread function obtained for the AFM probe close to a semiconductor surface (Strassburg, E.; Boag, A.; and Rosenwaks, Y. *Rev. Sci. Instrum*. **2005**, 76, 083705). We estimate the full-width-at-half-maximum (FWHM) of the point spread function to be ~ 25 nm in our case. Therefore, the measured SPV for the nanowires with the smallest diameters (~ 30 nm) might be an underestimation of the real value of SPV; this effect, however, is not expected to be significant, since the FWHM of the spread function is still comparable to the smallest nanowire diameter. We note that this effect does not change our observation that the SPV (and the surface state density) increases as the diameter decreases (see the text), i.e. such a diameter dependence would be even more significant if the AFM tip effect is included.

29. Meyer, B. K.; Alves, H.; Hofmann, D. M.; Kriegseis, W.; Forster, D.; Bertram, F.; Christen, J.; Hoffmann, A.; Strassburg, M.; Dworzak, M.; Haboeck, U.; Rodina, A. V. *Phys Status Solidi B* **2004,** 241, 231-260.

30. Kasap, S., *Springer Handbook of Electronic And Photonic Materials*. Springer: New York, 2006.

31. Chang, P. C.; Lu, J. G. *Appl. Phys. Lett.* **2008,** 92, 212113.

32. Allen, J. E.; Hemesath, E. R.; Perea, D. E.; Lensch-Falk, J. L.; Li, Z. Y.; Yin, F.; Gass, M. H.; Wang, P.; Bleloch, A. L.; Palmer, R. E.; Lauhon, L. J. *Nat Nanotechnol* **2008,** 3, 168-173.

33. Lagowski, J.; Sproles, E. S.; Gatos, H. C. *J. Appl. Phys.* **1977,** 48, 3566-3575.

34. Shih, T.; Winkler, M. T.; Voss, T.; Mazur, E. *Appl Phys a-Mater* **2009,** 96, 363-367.

35. Malkova, N.; Ning, C. Z. *Phys Rev B* **2006,** 74, 155308.

36. Lin, K. F.; Hsieh, W. F. *J Phys D Appl Phys* **2008,** 41, 215307.

37. Agrawal, R.; Peng, B.; Gdoutos, E. E.; Espinosa, H. D. Nano Lett. **2008**, 8, 3668-3674

38. Chiou, J. W.; Kumar, K. P. K.; Jan, J. C.; Tsai, H. M.; Bao, C. W.; Pong, W. F.; Chien, F. Z.; Tsai, M. H.; Hong, I. H.; Klauser, R.; Lee, J. F.; Wu, J. J.; Liu, S. C. *Appl. Phys. Lett.* **2004,** 85, 3220-3222.

39. Surface effects are minimized when most of the acceptor-type surface states are neutralized, which is indicated by a large SPV (close to the value of surface barrier height). Close to the metal junction, SPV decreases [Fig. 4 (b)], suggesting that surface effects become more significant in this region. However, SPV still remains larger than 0.1 V even at the edge of the metal electrode. For the smallest-diameter nanowire, where the surface effects are the strongest, this SPV corresponds to a τ_{sur} ~ 190 ps, which is larger than the bulk lifetime, indicating that bulk effects are still more significant in limiting the hole transport.

40. Shikler, R.; Fried, N.; Meoded, T.; Rosenwaks, Y. *Phys Rev B* **2000,** 61, 11041-11046.

41. The extension of the space-charge region along the nanowire channel can modify the measured surface potential profile close to the metal junction. Additionally, the contributions from KPFM tip-sample interactions can have an impact, as mentioned in Ref. 28. However, the space-charge region in ZnO nanowires with comparable doping levels does not extend into the nanowire channel region at bias lower than 10 V [Hwang, J.-S., Donatini, F., Pernot, J., Thierry, R., Ferret, P., and Dang, L. S., Nanotechnology **2011**, 22, 475704]. Also the spatial extension of the KPFM tip point spread function, which describes the tip-sample interactions, was estimated to be ~ 25 nm (Ref. 28), significantly smaller than L_D and within the experimental errors. Furthermore, the SPV profile was obained by subtracting the surface potential measured in the dark from that measured under the global optical excitation. This subtraction is expected to decrease/minimize the contributions of the space-charge region and tip-sample interactions. We note that, under the low-level optical excitation, the dimension of the space-charge region is expected to remain unchanged.

Table I

Bandgap	Dielectric constant (ϵ)	Electron (hole) effective mass	Electron (hole) mobility: μ_n (μ_p)	Donor concentration
3.33 eV	8.66	0.24 (0.8) m_0	100 (34) cm^2/Vs	10^{19} cm^{-3}

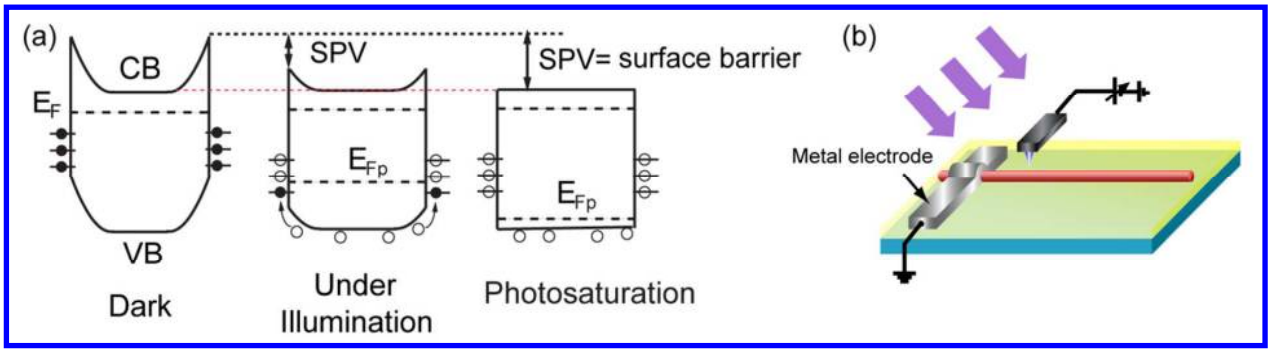

Figure 1 (a) Schematic cross-sectional band diagrams of a nanowire in the dark and under an optical illumination, with E_{Fp} representing the hole quasi-Fermi level under the optical illumination; (b) schematic experimental setup of the surface photovoltage measurements. CB and VB in (a) represent the conduction and the valence bands, respectively.

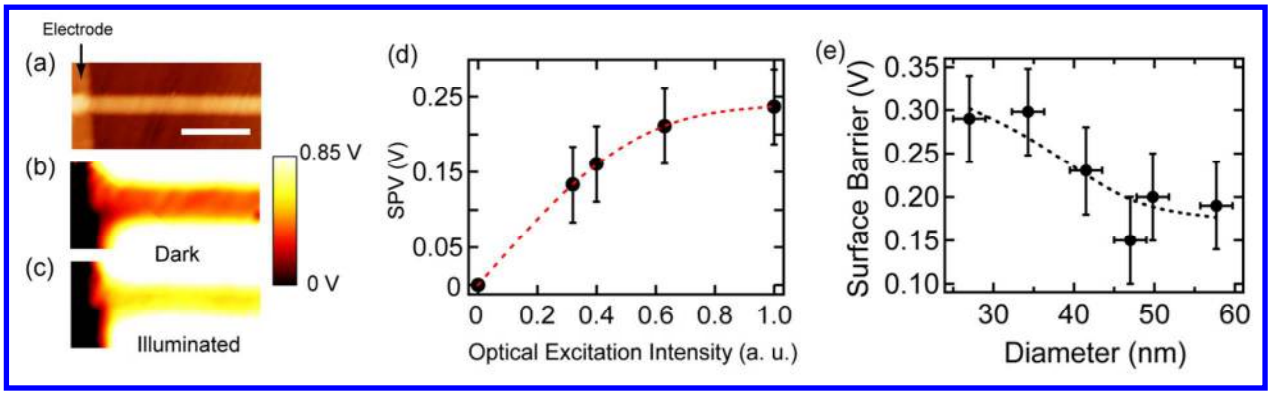

Figure 2 (a) Topography image of a ZnO nanowire attached to a metal electrode; surface potential maps of the nanowire (b) in the dark and (c) under the optical illumination; (d) measured SPV (solid circles) as a function of optical excitation intensity; (e) measured surface potential barrier (solid circles) height as a function of nanowire diameter. Dashed lines in (d) and (e) are spline interpolations as guide of the eye. Scale bar in (a): 0.5 μm.

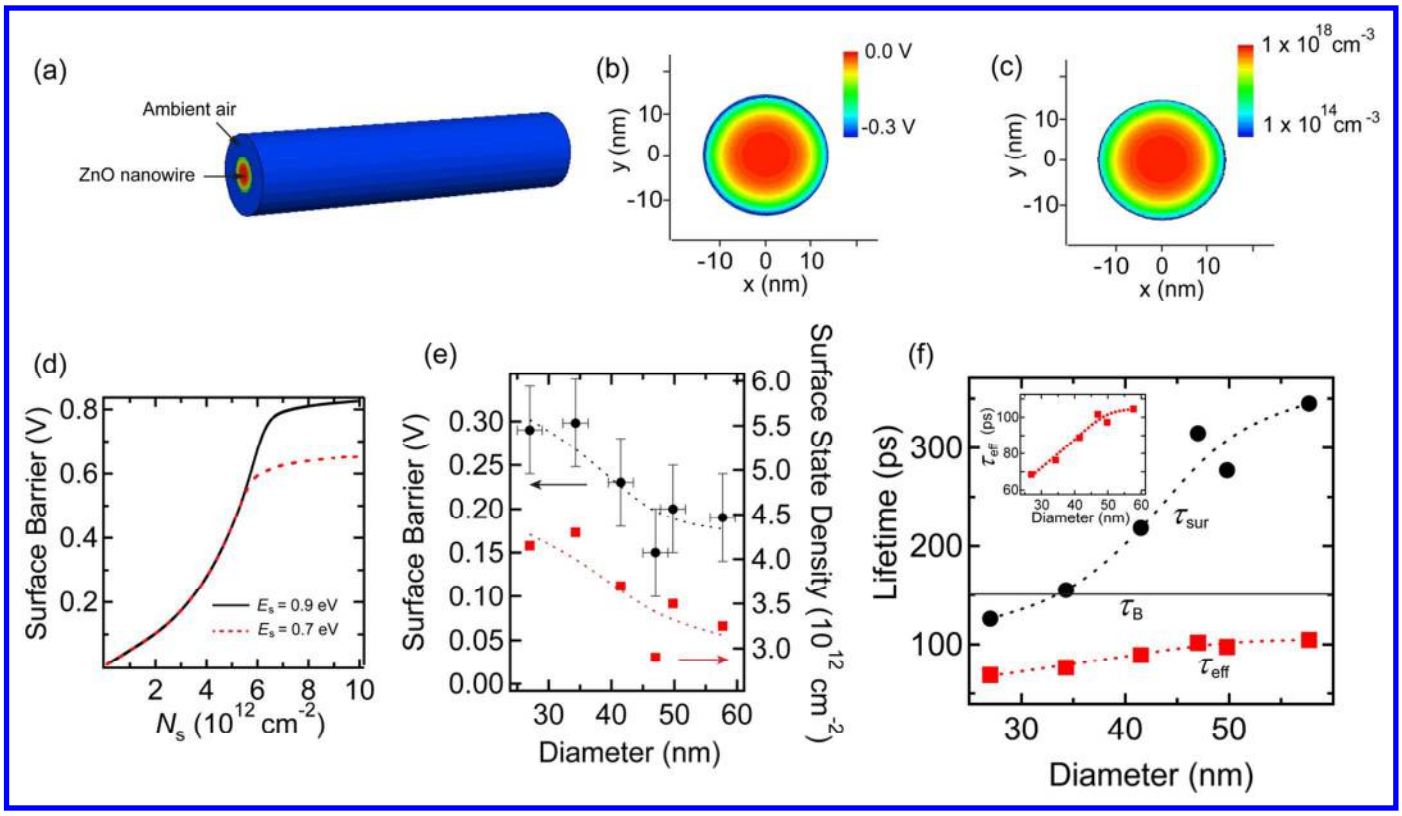

Figure 3 (a) Three-dimensional (3D) view of the calculated electrostatic potential of a 27 nm-diameter ZnO nanowire surrounded by ambient air; cross-sectional views of (b) potential and (c) electron density; (d) calculated surface potential barrier height for a 27 nm-diameter ZnO nanowire as a function of surface state density with the surface state energy levels at 0.9 eV (solid line) and 0.7 eV (dashed line) below the conduction band; (e) surface state density (solid squares) determined from the experimentally measured surface potential barrier height (solid circles) as a function of nanowire diameter; (f) calculated surface carrier lifetime (solid circles), τ_{sur}, and total lifetime (solid squares), τ_{eff}, as functions of nanowire diameter, with the inset showing a plot of τ_{eff} at various diameters. Dashed lines in (e) and (f) are spline interpolations.

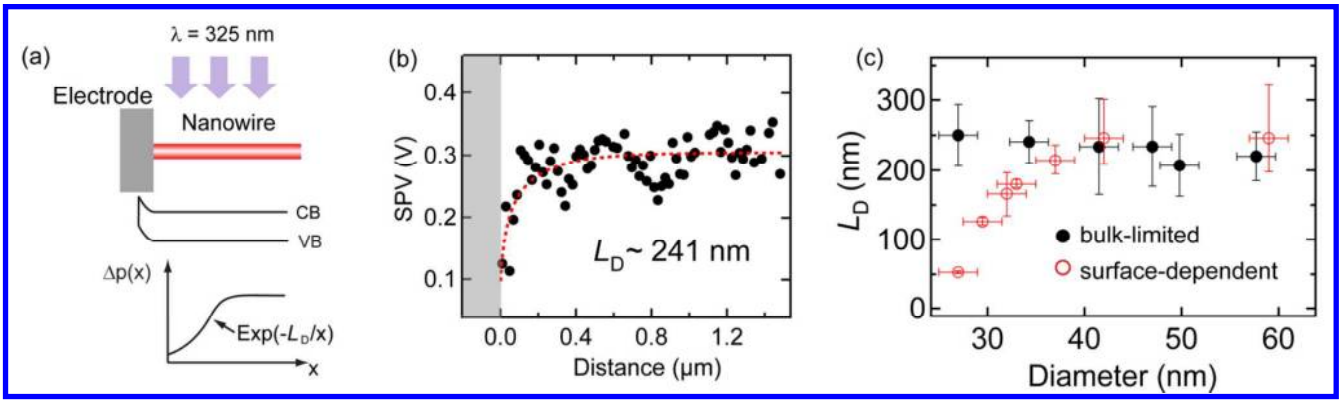

Figure 4 (a) Schematics of the measurement of bulk-limited L_D; (b) SPV (solid circles) spatial variations along a nanowire close to the metal junction, with the shaded region representing the metal electrode and the dashed line representing the fitting using the equation (5); (c) bulk-limited (solid circles) and surface-dependent (open circles) L_D as functions of nanowire diameter. The surface-dependent L_D is re-plotted from Ref. 8.

TOC Graphic

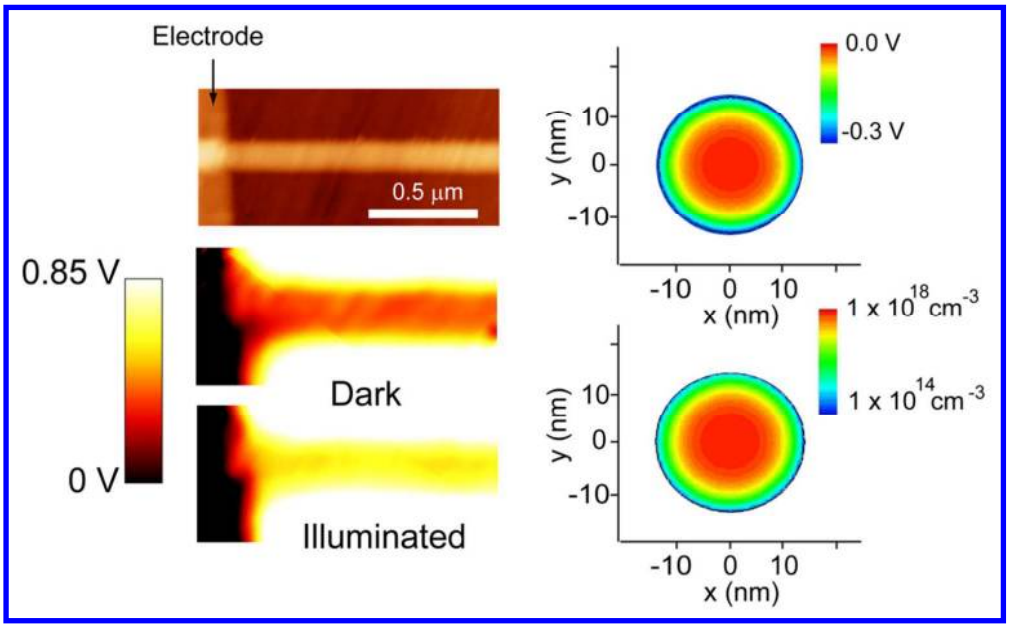
Electrode
0.5 μm
0.85 V
0 V
Dark
Illuminated
y (nm)
x (nm)
10
0
-10
0.0 V
-0.3 V
1 x 10^18 cm^-3
1 x 10^14 cm^-3

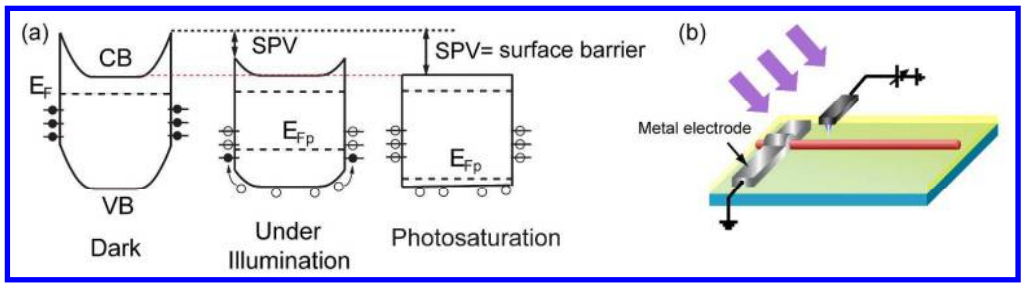

325x85mm (300 x 300 DPI)

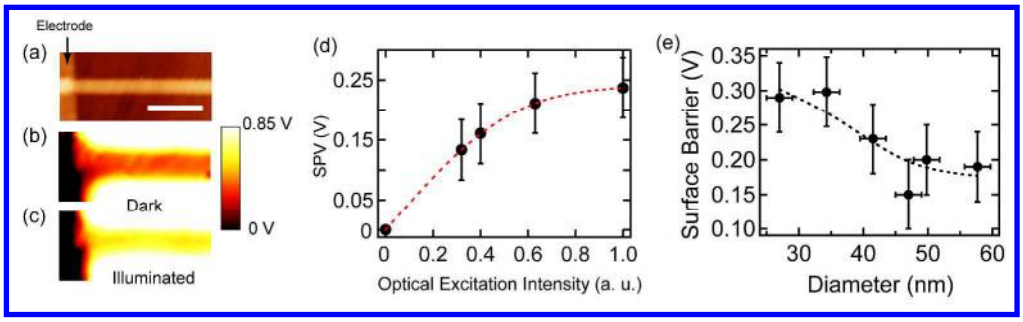

370x110mm (300 x 300 DPI)

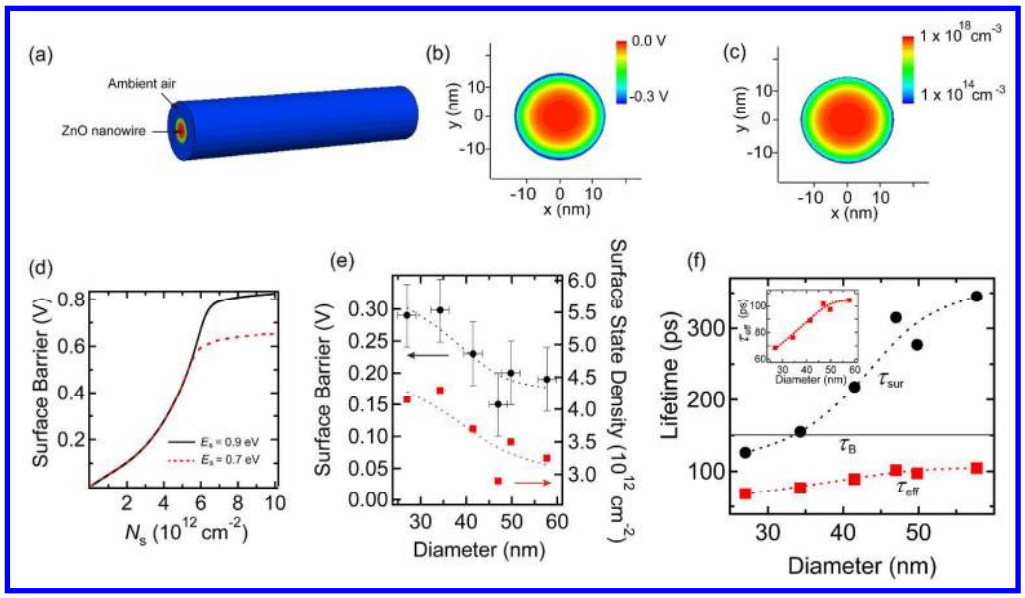

632x362mm (300 x 300 DPI)

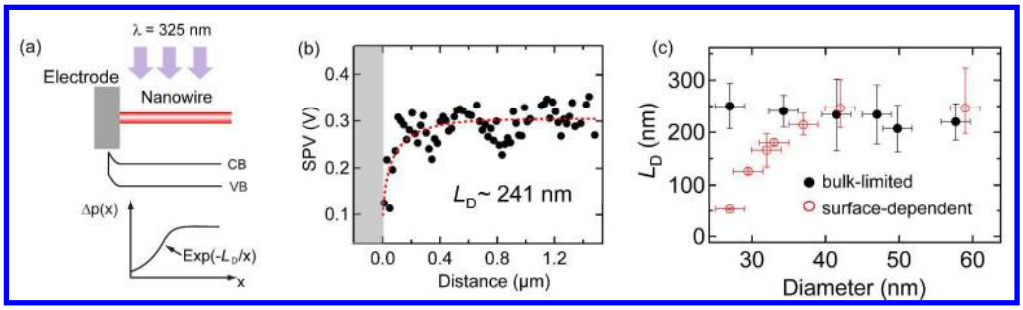

471x135mm (300 x 300 DPI)

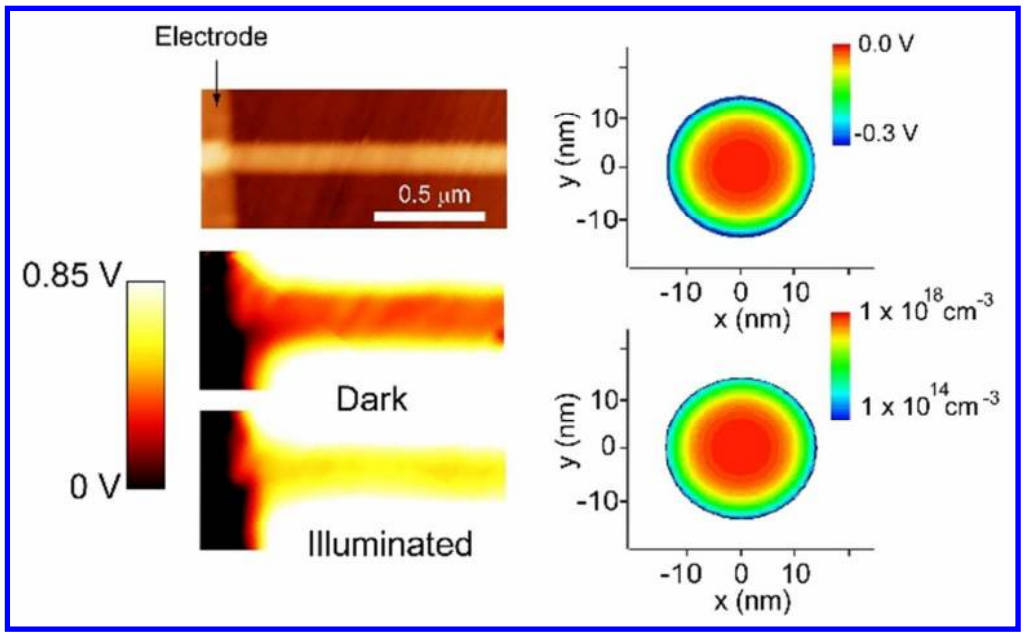

56x34mm (300 x 300 DPI)